



**Showcasing research from Professor Coulembier's laboratory, University of Mons, Mons, Belgium.**

CO<sub>2</sub>-binding alcohols as potential candidates for poly(vinyl chloride) upcycling

By combining waste CO<sub>2</sub> and PVC, Dr Olivier Coulembier and co-workers open new avenues for transforming two major pollutants into functional and valuable materials.

Image reproduced by permission of Coulembier Olivier from *Polym. Chem.*, 2025, **16**, 2923.

**As featured in:**



See Olivier Coulembier *et al.*, *Polym. Chem.*, 2025, **16**, 2923.



Cite this: *Polym. Chem.*, 2025, **16**, 2923

## CO<sub>2</sub>-binding alcohols as potential candidates for poly(vinyl chloride) upcycling†

Juliette Delcorps, Emna Ben Ayed and Olivier Coulembier \*

Despite the increasing global production of poly(vinyl chloride) (PVC), its recycling remains a major challenge, primarily due to its high chlorine content and limited compatibility with conventional recycling processes. This study explores the use of 1,5,7-triazabicyclo[4.4.0]dec-5-ene (TBD)-based CO<sub>2</sub>-binding alcohols (CO<sub>2</sub>BALs) as nucleophiles for PVC functionalization, aiming to enhance its upcycling potential. The impact of solvent polarity, CO<sub>2</sub>BAL conversion, and reaction time on the substitution-to-elimination ratio was systematically investigated. Although the degree of substitution remained below 10 wt%, a promising S<sub>N</sub>2/E2 selectivity of 94/6 was achieved. The functionalized materials were characterized using <sup>1</sup>H NMR, FT-IR, SEC, and TGA, confirming the successful grafting of carbonate moieties and highlighting thermal stability trends. While CO<sub>2</sub>BAL stabilization in polar solvents may limit reactivity, alternative approaches, such as flow chemistry, are currently under consideration to improve substitution efficiency. This work provides new insights into CO<sub>2</sub>-based strategies for PVC modification, bridging the gap between polymer upcycling and sustainable chemistry.

Received 8th April 2025,  
Accepted 11th May 2025

DOI: 10.1039/d5py00350d

rsc.li/polymers

### Introduction

With a global annual production of 45 million metric tons in 2022 and a projected increase to 65 million metric tons by 2030,<sup>1</sup> poly(vinyl chloride) (PVC) ranks as the third most produced polymer worldwide, following polyethylene (PE) and polypropylene (PP).<sup>2</sup> Its widespread use makes it a key target for the scientific community recycling efforts. Despite its reputation as a challenging material to recycle, Europe has seen significant progress in this area through initiatives such as Vinyl2010 and VinylPlus.<sup>3</sup> These programs have driven an impressive increase in PVC recycling, from just 18 000 tons in 2004 to 264 000 tons in 2010, and further to 731 000 tons in 2020. Projections suggest this figure could reach 1 million tons per year by 2030.<sup>4–6</sup> However, with an annual production of 6.5 million tons across the EU-27, Norway, Switzerland, and the United Kingdom,<sup>2</sup> the current recycling rates leave room for considerable improvement.

Two main approaches are currently employed for large-scale PVC recycling, *i.e.* mechanical recycling and feedstock (or chemical) recycling.<sup>4–7</sup> Unfortunately, both methods face significant limitations. Mechanical recycling requires thoroughly sorted and homogeneous PVC waste to produce a material

with properties comparable to the original polymer.<sup>5–7</sup> This stringent requirement complicates waste management, and the process itself often degrades polymer chains, leading to a loss of physical and mechanical properties that restrict the applications of the recycled material.<sup>5</sup> Feedstock recycling, on the other hand, is hindered by PVC's high chlorine content. This method typically involves thermal treatments, during which the easily broken C–Cl bond releases chlorinated derivatives (Fig. 1a). If not effectively captured, these emissions can cause equipment corrosion and air pollution. Moreover, dehydrochlorination generates conjugated polyene sequences that may undergo cyclization to form regular and chlorinated aromatic compounds, further increasing the environmental burden of feedstock recycling.<sup>7</sup> The recovery of chlorine from PVC and other chlorinated polymers, such as polyvinylidene chloride (PVDC), is thus crucial to their recycling process.<sup>8–10</sup>

To overcome the limitations of traditional recycling methods, innovative approaches such as biological and electrochemical recycling,<sup>8</sup> as well as chemical upcycling,<sup>11</sup> have been explored and warrant further research.<sup>5,12</sup> Among these, chemical upcycling through nucleophilic substitution has garnered significant attention.<sup>13</sup> However, the efficiency of these substitution reactions is influenced by a variety of factors, including the leaving group properties, the polymer structure, and the reaction environment.<sup>14–16</sup> For instance, while chlorine is a modest leaving group that can undergo substitution and elimination reactions under various conditions,<sup>17</sup> product selectivity remains a challenge due to the competition between these pathways. Factors such as solvent polarity, nucleophile

Laboratory of Polymeric and Composite Materials, Centre of Innovation and Research in Materials and Polymers, University of Mons, Place du Parc 23, 7000 Mons, Belgium. E-mail: [olivier.coulembier@umons.ac.be](mailto:olivier.coulembier@umons.ac.be)

† Electronic supplementary information (ESI) available. See DOI: <https://doi.org/10.1039/d5py00350d>



**Fig. 1** Chlorine reactivity and selectivity in PVC modifications: (a) common reactivities of C–Cl bonds in PVC, (b) nucleophile-dependent substitution (S<sub>N</sub>2) and elimination (E2) ratios (I<sup>-</sup> in DMF at 60 °C, SCN<sup>-</sup> in DMF at 100 °C, HO<sup>-</sup> in DMF at 21 °C, N<sub>3</sub><sup>-</sup> in DMF at 100 °C, phthalimide anion in DMF at 60 °C, ethylenediamine at 75 °C in bulk, 1-octanethiol/K<sub>2</sub>CO<sub>3</sub> in DMF at 40 °C), and (c) enhanced selectivity using CO<sub>2</sub>BALs in our work (R = Decyl).

identity, temperature, and nucleophile concentration play a critical role in directing the reaction.<sup>17</sup> Polar aprotic solvents like dimethylformamide (DMF) have been shown to favor substitution over elimination, while higher temperatures tend to promote elimination.<sup>18,19</sup> Similarly, less basic nucleophiles increase substitution selectivity,<sup>17</sup> offering avenues for tailoring reaction conditions to improve outcomes.

Substitution reactions with nucleophiles offer the potential to convert PVC into new polymeric materials for specialized applications, including catalysis,<sup>20,21</sup> separations,<sup>22,23</sup> and antimicrobial polymers.<sup>24</sup> Nevertheless, such transformations often face practical limitations due to incomplete dechlorination and competition with elimination, leading to residual chlorine atoms and alkenes that can alter polymer properties.<sup>25</sup> These challenges underscore the need for innovative strategies to enhance both the efficiency and selectivity of substitution reactions, as demonstrated by recent studies.<sup>26</sup>

Optimizing these reaction parameters could enable the development of versatile and sustainable recycling methods for PVC. For instance, a variety of nucleophiles, including iodide anion, hydroxide, azide, and thiocyanate, have been explored for PVC substitution reactions (Fig. 1b).<sup>19</sup> Thiols have also been employed, with Lu *et al.* achieving partial substitution of PVC chlorine atoms using potassium carbonate and *N,N*-diisopropylethylamine.<sup>27</sup> Additionally, amination of PVC has enabled its upcycling into carbon dioxide absorbents, as demonstrated by Sneddon *et al.*<sup>28</sup> However, while the use of nucleophiles for PVC modification has been extensively

studied, research on employing carbonates as nucleophiles remains notably sparse. This gap is particularly surprising given the potential for carbonates to provide functionalized PVC materials with unique properties. Furthermore, although substitution reactions are often accompanied by elimination processes, the latter is either underreported or dominates in most studies,<sup>16</sup> underscoring the need for approaches that favour selective substitution over elimination.

In this work, we aimed to functionalize PVC using 1,5,7-triazabicyclo[4.4.0]dec-5-ene (TBD)-based CO<sub>2</sub>-binding alcohol-derived materials (CO<sub>2</sub>BALs), previously developed for the synthesis of “simple” dialkyl carbonates (Fig. 1c).<sup>29</sup> The effects of temperature, solvent polarity, CO<sub>2</sub>BAL conversion, and reaction time were systematically studied to evaluate their impact on both the degree of substitution and the substitution-to-elimination ratio. Although substitution levels higher than 10 wt% were not achieved in optimal conditions, this result makes the CO<sub>2</sub>BAL approach particularly appealing, as the nature of the by-product is a TBD·HCl salt, which is harmless. However, for future investigations, it will be necessary to consider other functionalization strategies, such as flow chemistry.

## Results and discussion

Carbon dioxide-binding organic liquids (CO<sub>2</sub>BOLs) are an innovative class of materials formed by combining alcohols

with liquid organic bases, such as amidines or guanidines.<sup>30–33</sup> These systems are capable of binding CO<sub>2</sub> through reversible interactions, making them highly versatile for applications in CO<sub>2</sub> capture and utilization.

CO<sub>2</sub>BOLs form intermediates that can act as nucleophiles in substitution reactions,<sup>29,34–36</sup> opening new avenues for polymer transformations and upcycling strategies. Among the organic bases used in CO<sub>2</sub>BOLs, 1,5,7-triazabicyclo[4.4.0]dec-5-ene (TBD) has recently garnered particular attention.<sup>37</sup> TBD-based CO<sub>2</sub>BOLs exhibit a unique ability to promote selective S<sub>N</sub>2 (bimolecular nucleophilic substitution) reactions with primary and secondary iodo-alkanes.<sup>29</sup> This selectivity primarily arises from the formation of a TBD·H<sup>+</sup> guanidinium cation during the reaction, which interacts with and stabilizes the iodine ion released as the leaving group in the S<sub>N</sub>2 process. By minimizing competing reactions such as elimination or base quaternization, this mechanism enables highly efficient and controlled transformations.

Building on these properties, this study extends the application of TBD-based CO<sub>2</sub>BOLs beyond small-molecule transformations to the upcycling of poly(vinyl chloride) (PVC), a widely used polymer with significant recycling challenges. To better highlight the improvements introduced in this work, several key aspects are compared in Table 1, showcasing the differences between TBD-based CO<sub>2</sub>BOLs used for small-molecule synthesis (*cf.* ref. 29) and their application in PVC recycling. As far as the environmental impact is concerned, it was hypothesized that these systems could limit the release of chloride ions during both dechlorination and dehydrochlorination (Fig. 2). By leveraging the chloride-trapping ability of TBD·H<sup>+</sup>, this approach seeks to reduce the formation of toxic by-products while enhancing substitution efficiency on the PVC backbone. Moreover, this work underscores the dual sustainability of the proposed method: integrating CO<sub>2</sub> into the reaction process transforms this abundant greenhouse gas into a valuable resource for polymer modification. This innovative use of CO<sub>2</sub> not only aligns with broader goals in carbon capture and utilization but also addresses critical challenges in PVC recycling.

To better reflect the versatility of the systems explored in this study, the term CO<sub>2</sub>BALs (“CO<sub>2</sub>-binding alcohols”) is pro-



Fig. 2 Trapping of chloride by guanidinium TBD·H<sup>+</sup> during (a) dechlorination (S<sub>N</sub>2) and (b) dehydrochlorination (E2) reactions.

posed to describe alcohol-based systems that extend beyond the liquid-phase CO<sub>2</sub>BOLs typically described in the literature. This broader definition emphasizes the adaptability of CO<sub>2</sub>BALs in enabling sustainable and efficient polymer transformations.

### Thermal properties of CO<sub>2</sub>BALs: melting points and degradation

In developing a method to functionalize PVC using CO<sub>2</sub>BALs, a solvent-free approach was prioritized to enhance the environmental sustainability of the process and minimize waste generation. Such an approach requires both reactants to be in a compatible physical state to ensure effective interaction. For PVC, this means operating above its Vicat softening temperature (~92 °C)<sup>38</sup> but below its thermal degradation threshold (~250 °C).<sup>39</sup> The CO<sub>2</sub>BALs, on the other hand, must remain liquid under these conditions, as this enhances their ability to mix with the polymer and facilitates reactivity.

To evaluate the feasibility of these conditions, the melting points and thermal stability of CO<sub>2</sub>BALs were studied. A series

Table 1 Main differences, environmental impact and major innovation between TBD-based CO<sub>2</sub>BOLs used for small-molecule synthesis (ref. 29) and this work

Criteria	Ref. 29	This work
Main objective	Synthesis of dialkyl carbonates <i>via</i> S <sub>N</sub> 2 with TBD-based CO <sub>2</sub> BOLs	Upcycling of PVC with CO <sub>2</sub> BOLs for sustainable valorization
Main substrates	Primary and secondary alkyl iodides	PVC secondary methine chlorides
Final product	Dialkyl carbonates	Carbonate-modified PVC through an almost exclusively S <sub>N</sub> 2 process and a limited HCl-liberating E2 reaction
Reaction temperature	21–65 °C	21 °C (optimal conditions)
Solvents used	Acetonitrile or solvent-free condition	DMF (optimal conditions)
Environmental impact	Green alternative to toxic metal-based methods	Plastic waste valorization, reduction of HCl waste by-product by an exclusive TBD·HCl benign salt production
Major innovation	Guanidinium-assisted S <sub>N</sub> 2 ion-pair process	Extension to polymers, contribution to PVC recycling by CO <sub>2</sub> valorization

of TBD alkylcarbonate salts were prepared by mixing equimolar amounts of alcohol and TBD in bulk, as previously detailed by us.<sup>29</sup> Mixtures were then heated to a constant temperature and exposed to CO<sub>2</sub> ( $p_{\text{CO}_2} = 0.2$  bar) under vigorous stirring (500 rpm). The temperature was maintained at 50 °C for methanol, ethanol, and 1-propanol, while 90 °C was used for 1-butanol, 1-hexanol, 1-octanol, and 1-decanol (Fig. S1, S3, S5, S7, S9, and S11†). The thermal properties of the obtained CO<sub>2</sub>BALs were evaluated by determining their melting points, which are influenced by the length of the alkyl chain. As shown in Fig. 3, with the exception of the TBD butylcarbonate salt (which remains a viscous liquid with a melting temperature of 13.5 °C), all other CO<sub>2</sub>BALs are solid at room temperature. The melting points follow a clear trend: they decrease with the length of the alkyl chain down to a minimum for the 1-butanol-based salt, after which they slightly increase for longer chains. These results were compared to those of 1,8-diazabicyclo[5.4.0]undec-7-ene (DBU)- and 1,1,3,3-tetramethylguanidine (TMG)-based CO<sub>2</sub>BALs,<sup>33</sup> with the latter exhibiting negative melting points across all alkyl chain lengths. Notably, the melting points of the TBD-based CO<sub>2</sub>BALs are generally higher than those of DBU-based salts, particularly for shorter alkyl chains such as methanol, ethanol, and 1-propanol. This suggests that the TBD salts form more stable crystalline structures compared to DBU and TMG salts. This thermal behavior is significant when considering the conditions required for the upcycling of PVC, as the melting point influences both the stability and reactivity of the CO<sub>2</sub>BALs during polymer functionalization.

Initially encouraged by the relatively high melting points of CO<sub>2</sub>BALs derived from methanol, ethanol, and 1-propanol, we faced a critical limitation when examining their thermal stability. Thermogravimetric analyses (TGA) revealed that the degradation onset temperatures (T<sub>5%</sub>) of these salts are consistently close to their melting points (*ca.* 80–85 °C, Fig. S2, S4, and S6†), excluding their use in liquid form at temperatures compatible with PVC's Vicat softening point. Furthermore, the TGA data showed that the degradation temperatures of CO<sub>2</sub>BALs are independent of alkyl chain length, falling within



**Fig. 3** Melting points of TBD-based CO<sub>2</sub>BALs as a function of the alkyl chain length, compared with the melting points of DBU- and TMG-based CO<sub>2</sub>BALs. Thermal data for DBU (in orange) and TMG (in purple) are adapted from ref. 33.

a narrow range of 80–90 °C (Fig. S2, S4, S6, S8, S10, S12 and S14†).

To gain deeper insight into the thermal behavior of CO<sub>2</sub>BALs, we sought to determine the activation energy ( $E_a$ ) and pre-exponential factor ( $A$ ) by applying the Arrhenius equation across a broad temperature range (40–110 °C). This required selecting a CO<sub>2</sub>BAL with a melting point sufficiently distinct from its T<sub>5%</sub> to ensure reliable thermal measurements. The 1-decanol-based CO<sub>2</sub>BAL emerged as a good candidate, with a melting point of 31.5 °C and a degradation onset temperature of 86.4 °C. These properties provided a stable and practical platform for assessing thermal stability and reactivity. It should also be noted that, as previously reported,<sup>29</sup> the longer alkyl chain of 1-decanol poses a barrier to achieving quantitative carbonate conversion. The synthesis of the corresponding CO<sub>2</sub>BAL used here was indeed limited to ~80% conversion, as determined by <sup>1</sup>H NMR analysis (Fig. S13c†). Despite this slight limitation, the thermal properties of this compound made it a good choice for the subsequent experiments.

In the simplest approach, the decarboxylation reaction rate constant for the 1-decanol-based CO<sub>2</sub>BAL,  $k$ , can be calculated according to the eqn (1):

$$\ln\left(\frac{[\text{CO}_2\text{BAL}]_0}{[\text{CO}_2\text{BAL}]_t}\right) = k \cdot t \quad (1)$$

where  $[\text{CO}_2\text{BAL}]_0$  and  $[\text{CO}_2\text{BAL}]_t$  represent the concentration in CO<sub>2</sub>BAL at time 0 and  $t$  minutes, respectively. The decarboxylation rate constant,  $k$ , can, therefore be calculated from the gradient for each semi-log plots at the different selected temperatures (Fig. 4a). Examination of the liberation of CO<sub>2</sub> from the TBD-based salt under a constant nitrogen flow ( $p_{\text{N}_2} = 0.2$  bar), reveals that it takes 10 h to achieve ~50% degradation at 40 °C, whereas an almost complete degradation occurs within 0.3 h at 110 °C. The Arrhenius plot is then applied to calculate



**Fig. 4** (a) Decarboxylation kinetics of 1-decanol-based CO<sub>2</sub>BAL at different temperatures and (b) corresponding Arrhenius plot.

the activation energy (Fig. 4b),  $E_a$ , and the pre-exponential factor,  $A$ , according to the eqn (2):

$$\ln k = \ln A - \frac{E_a}{R \cdot T} \quad (2)$$

where  $R$  is the universal gas constant ( $8.3144 \text{ J mol}^{-1} \text{ K}^{-1}$ ).

The activation energy ( $E_a$ ) and pre-exponential factor ( $A$ ) obtained for the 1-decanol-based  $\text{CO}_2\text{BAL}$  ( $62 \text{ kJ mol}^{-1}$  and  $2.4 \times 10^7 \text{ min}^{-1}$ ) fall within the typical range observed for first-order reactions involving complex organic transformations. For instance, Moreno *et al.* reported a  $E_a$  values of  $58.7\text{--}70.5 \text{ kJ mol}^{-1}$  for cannabinoid decarboxylation,<sup>40</sup> illustrating that the thermal behavior of the 1-decanol-based  $\text{CO}_2\text{BAL}$  is comparable to other thermally activated systems. While this moderate  $E_a$  reflects a certain degree of thermal stability, it also indicates that degradation becomes non-negligible at elevated temperatures. Combined with the relatively low degradation onset temperature ( $75\% = 86.4 \text{ }^\circ\text{C}$ ), this limits the practical use of the  $\text{CO}_2\text{BAL}$  in bulk conditions, particularly for PVC functionalization near its Vicat softening temperature ( $\sim 92 \text{ }^\circ\text{C}$ ). These findings further justify transitioning to solution-phase reactions, where thermal constraints are minimized, allowing for more controlled and efficient reactivity.

### Reaction between PVC and $\text{CO}_2\text{BAL}$ s in solution

Unlike high-temperature bulk processes, solution-phase methods offer greater flexibility in selecting both the reaction temperature and the polarity of the medium. For PVC, only tetrahydrofuran (THF, dipole moment =  $1.75 \text{ D}$ ), *N,N*-dimethylformamide (DMF, dipole moment =  $3.82 \text{ D}$ ), and methyl ethyl ketone (MEK, dipole moment =  $2.81 \text{ D}$ ) have been considered to investigate the ability of  $\text{CO}_2\text{BAL}$  to react with PVC at room temperature.<sup>41–44</sup> While THF is known to dissolve PVC completely, it was directly discarded due to its inability to solubilize  $\text{CO}_2\text{BAL}$  of 1-decanol (conv.  $\sim 80\%$ ) whatever its concentration. DMF and MEK, which exhibit satisfactory PVC dissolution performances and known to perfectly solubilize  $\text{CO}_2\text{BAL}$ s, have then been compared.

Before initiating any reaction, the absolute number-average molar mass of PVC was determined. The theoretical number-average molar mass ( $M_{n,\text{th}}$ ) provided by Sigma is estimated at  $48\,000 \text{ g mol}^{-1}$ . Experimentally, Size Exclusion Chromatography (SEC) was performed using a polystyrene (PS) standard calibration in THF at  $25 \text{ }^\circ\text{C}$ , with the Mark–Houwink relationship applied for both PS and PVC ( $[\eta] = KM^a$ , where  $K_{\text{PS}} = 1.1 \times 10^{-4} \text{ dL g}^{-1}$  and  $a_{\text{PS}} = 0.725$  for PS;  $K_{\text{PVC}} = 1.658 \times 10^{-4} \text{ dL g}^{-1}$  and  $a_{\text{PVC}} = 0.76$  for PVC).<sup>45</sup> This analysis yielded an experimental number-average molar mass ( $M_{n,\text{SEC}}$ ) of  $41\,400 \text{ g mol}^{-1}$  and a dispersity value ( $D_M = M_w/M_n$ ) of 2.2. Prior to correction, the relative  $M_{n,\text{SEC}}$  was  $63\,500 \text{ g mol}^{-1}$ .

To limit the significance of elimination reactions, which typically play a major role in the  $\text{S}_{\text{N}}2\text{--E}2$  competition with PVC,<sup>19,27,28</sup> reactions were performed at  $21 \text{ }^\circ\text{C}$  by reacting a  $\text{CO}_2\text{BAL}$  of 1-decanol (conv.  $\sim 80\%$ ) in a PVC solution ( $[\text{PVC}]_0 = 0.7 \text{ mmol L}^{-1}$ ) for an initial  $[\text{Cl}]_0\text{--}[\text{CO}_2\text{BAL}]_0$  molar ratio of 1. Even though MEK is capable of perfectly dissolving both PVC

and the  $\text{CO}_2\text{BAL}$  of 1-decanol individually, their combination in this solvent and under the applied concentration conditions renders the  $\text{CO}_2\text{BAL}$  of 1-decanol insoluble. Under vigorous stirring, and after several hours, the insolubilization of  $\text{CO}_2\text{BAL}$  gradually diminishes, eventually disappearing and leaving behind an insoluble black precipitate that does not dissolve in any of the organic solvents used. In our opinion, such a black insoluble precipitate is likely due to the formation of a polyacetylene-like structure, possibly resulting from the degradation of  $\text{CO}_2\text{BAL}$ , which releases 1-decanol and TBD into the solution. The free TBD, or the alkoxide formed by deprotonation of 1-decanol by the guanidine, could then act as a base, promoting E2 elimination reactions on the PVC. Interestingly, the rate of insolubilization has been observed variable with the degree of  $\text{CO}_2\text{BAL}$  conversion, *i.e.*,  $\text{CO}_2\text{BAL}$ s of varying degrees of carbonate conversion. Two TBD decanol-based carbonate salts with different degrees of carbonate conversion were then prepared under  $\text{CO}_2$  by mixing equimolar amounts of 1-decanol and TBD at  $90 \text{ }^\circ\text{C}$  for different reaction times. This approach allowed us to prepare new  $\text{CO}_2\text{BAL}$ s with carbonate conversions of 50 and 75 mol% (Fig. S13a and b†). Note that a conversion of 75% corresponds to a salt composed of 75 mol% carbonate and 25 mol% TBD alkoxide. A TBD alkoxide (referred to as the “0% conversion”) also served as a reference for a  $\text{CO}_2\text{BAL}$  system entirely devoid of  $\text{CO}_2$ . These  $\text{CO}_2\text{BAL}$ s were then reacted with PVC previously dissolved in MEK ( $[\text{PVC}]_0 = 0.7 \text{ mmol L}^{-1}$ ) for a reaction time limited to 1 hour and a  $[\text{Cl}]_0\text{--}[\text{1-decanol}]_0 = 1$ .  $^1\text{H}$  NMR analyses of the three reactions reveal no apparent reaction with the  $\text{CO}_2\text{BAL}$  but a substantial increase in vinyl protons showing up at  $\delta = 5.5\text{--}6 \text{ ppm}$  (Fig. S15 and S16†). By integrating these protons relative to the CH–Cl signals of PVC ( $\delta = 4.35\text{--}4.65 \text{ ppm}$ ), the proportion of E2 elimination per chain ( $= 100 \times (I_{5.5\text{--}6}/2) / [(I_{5.5\text{--}6}/2) + I_{4.35\text{--}4.65}]$ ) rises with decreasing  $\text{CO}_2\text{BAL}$  conversion. Moreover, the relative  $M_{n,\text{SEC}}$  values also decrease accordingly, in agreement with the literature.<sup>46</sup> These trends are summarized in Fig. 5, which compares the proportion of E2 elimination with the corresponding  $M_{n,\text{SEC}}$  values. It should be



**Fig. 5** Influence of  $\text{CO}_2\text{BAL}$  carbonate conversion on the reaction outcome with PVC in MEK at  $21 \text{ }^\circ\text{C}$  ( $[\text{PVC}]_0 = 0.7 \text{ mmol L}^{-1}$ ,  $[\text{Cl}]_0\text{--}[\text{1-decanol}]_0 = 1$ , reaction time = 1 h). The relative  $M_{n,\text{SEC}}$  values (in orange) and the proportion of E2 elimination (in blue) are plotted as a function of the  $\text{CO}_2\text{BAL}$  carbonate conversion.

noted that for the sample obtained with CO<sub>2</sub>BAL 0% (*i.e.*, an equimolar mixture of 1-decanol and TBD), only the soluble fraction was analyzed by SEC, while the majority remained insoluble in the SEC eluent, likely due to a high unsaturation content.

To overcome the limitations observed in MEK, reactions were finally carried out at 21 °C in DMF, a solvent ensuring complete solubilization of both PVC and the CO<sub>2</sub>BAL of 1-decanol. Five functionalization reactions were performed in parallel for reaction times of 30 minutes, 1 hour, 2 hours, 18 hours, and 72 hours. Each reaction medium was subsequently precipitated, washed, and dried to ensure complete removal of decanol derivatives. <sup>1</sup>H NMR analyses revealed signals associated with the  $\alpha$ -methine proton of a decyl carbonate, which typically appears at  $\delta = 4.87$  ppm for alkyl carbonates and  $\delta = 4.97$  ppm for acyl carbonates.<sup>29,47</sup> In the present case, a signal was detected at approximately  $\delta = 4.76$  ppm, overlapping with the PVC methine protons, suggesting the formation of a decyl-based carbonate. Additionally, a triplet at  $\delta = 0.89$  ppm, corresponding to terminal methyl protons of decyl chains, confirmed the successful reaction of CO<sub>2</sub>BAL with PVC (Fig. 6a). Notably, vinyl proton signals ( $\delta = 5.5$ – $6$  ppm) first appeared at the 2-hour mark, corresponding to an S<sub>N</sub>2/E2 ratio of 94/6. Beyond this point, the selectivity shifted in favour of elimination, with S<sub>N</sub>2/E2 ratios decreasing to 54/46 after 18 hours and 38/62 after 72 hours. This shift was accompanied by a decrease in relative  $M_n$ SEC values, which initially increased from 63 500 g mol<sup>-1</sup> for PVC to over 89 000 g mol<sup>-1</sup> after 2 hours, before declining for longer reaction times (Fig. S17 and S18†). These observations suggest that prolonged reaction times lead to kinetic instability and the gradual release of free TBD into the reaction medium, promoting elimination over substitution.

The success of the reaction was further confirmed by Fourier Transform Infrared (FTIR) spectroscopy. The spectrum of the sample obtained after 2 hours of reaction exhibited a new absorption band at 1744 cm<sup>-1</sup>, attributed to the asymmetric stretching of the C=O bond. This frequency matches that observed for a model small molecule in our previous work (Fig. 6b).<sup>29</sup> Notably, no significant absorption bands corresponding to C=C stretching vibrations were detected, indicating that vinyl unsaturations formed *via* elimination remain below the FT-IR detection limit.

The sample obtained after 2 hours of reaction was further analyzed by thermogravimetric analysis (TGA) to accurately determine the mass fraction of grafted carbonate moieties and compared to the pristine PVC (Fig. 7). As expected, the thermogram of pristine PVC exhibits thermal stability up to 230 °C, beyond which rapid dehydrochlorination occurs, spanning the temperature range of 230 to 370 °C.<sup>48</sup> Between 375 and 525 °C, the degraded polyene structures undergo transformation into condensed aromatic hydrocarbons, eventually yielding infusible coke with a residual carbon content of approximately 6.8% at 650 °C. Three key differences were observed in the thermogram of modified PVC. First, an additional mass loss step appears at *ca.* 125 °C, attributed to the degradation of the

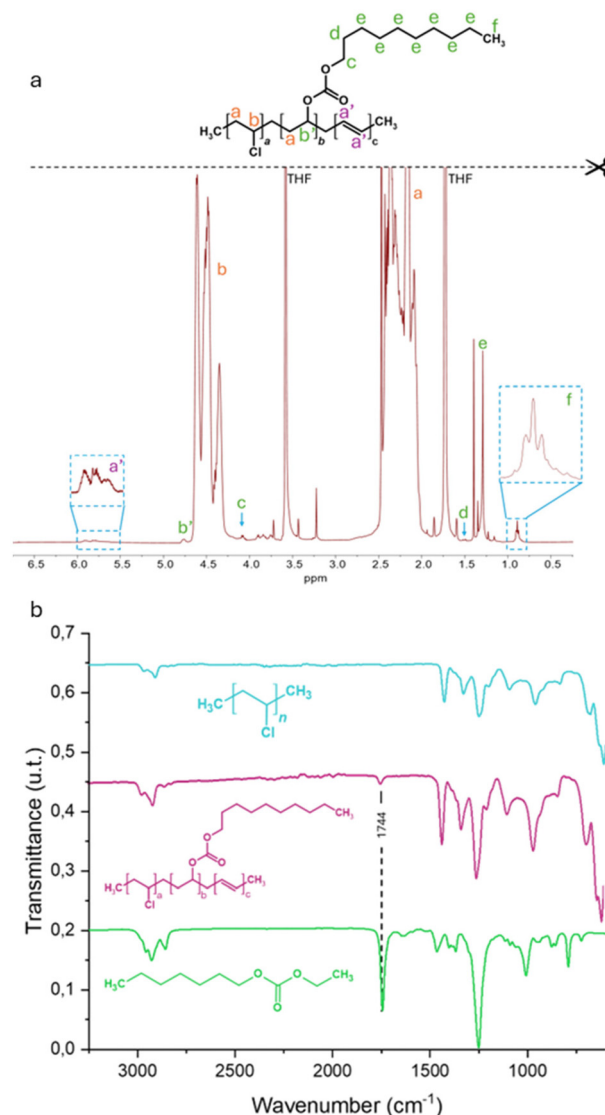


Fig. 6 (a) <sup>1</sup>H NMR (THF-d<sub>8</sub>, 500 MHz) of modified PVC (b) FT-IR of PVC (blue), modified PVC (purple), and a heptyl-ethyl carbonate (green) used in comparison and prepared as reported in ref. 29.

grafted carbonate groups. Second, the chlorinated backbone of PVC is destabilized upon functionalization, as evidenced by a shift in the dehydrochlorination onset temperature from 230 °C (pristine PVC) to approximately 180 °C. This phenomenon is well-documented in the literature.<sup>27,28,49,50</sup> Finally, the coke residue at 650 °C is slightly higher for modified PVC compared to pristine PVC, likely reflecting the small proportion of elimination reactions detected by <sup>1</sup>H NMR spectroscopy.

The limited grafting efficiency observed in DMF can be attributed to a combination of steric and electronic factors. CO<sub>2</sub>BALs are known to be significantly stabilized in highly polar solvents like DMF due to dipolar interactions,<sup>29</sup> which reduces their overall reactivity and may hinder efficient nucleophilic attack. In S<sub>N</sub>2 reactions, the substitution of the halogenated carbon is governed by both the dynamics and reactivity



Fig. 7 Thermal stability of pristine PVC (orange) and PVC modified with 1-decanol-based CO<sub>2</sub>BAL (conv. 80%) in DMF for 2 hours.

of the system.<sup>51</sup> Typically, S<sub>N</sub>2 reactions proceed *via* a backside attack, resulting in Walden inversion. However, the introduction of bulky substituents can sterically hinder this pathway, potentially favoring an S<sub>N</sub>2 frontside mechanism despite its slightly higher energetic cost. In the case of PVC, a statistical coil polymer with randomly distributed CH-Cl electrophilic sites, steric hindrance plays a crucial role in dictating the reaction pathway. The steric environment likely promotes frontside S<sub>N</sub>2 substitution, especially when assisted by a guanidinium ion-pair mechanism (Scheme 1).<sup>29</sup> The combination of CO<sub>2</sub>BAL stabilization in DMF and steric constraints on the PVC backbone could thus explain the observed limitation in grafting efficiency. Further investigations, such as a flow chemistry-driven reaction, are currently underway to explore alternative strategies aimed at improving reaction yields.



Scheme 1 Mechanism proposed for PVC substitution from CO<sub>2</sub>BAL by a frontside approach.

## Conclusions

Bulk-phase reactions revealed that CO<sub>2</sub>BALs undergo degradation under these conditions, necessitating the use of solution-phase functionalization for efficient PVC modification at 21 °C. Despite a moderate degree of substitution (<10 wt%) compared to some already existing and present in the introduction, this approach achieved a remarkable S<sub>N</sub>2 selectivity (94/6) while generating a single, benign by-product (TBD-HCl). Spectroscopic and thermal analyses confirmed the successful grafting of carbonate functionalities, though solvent effects influenced reaction efficiency. Specifically, the strong stabilization of CO<sub>2</sub>BALs in polar solvents like DMF reduced their nucleophilicity at room temperature, highlighting the need for alternative strategies to enhance substitution yields. Beyond PVC functionalization, this strategy holds broader environmental benefits. The use of CO<sub>2</sub>BALs introduces a novel approach for integrating CO<sub>2</sub> into polymer modifications, aligning with circular economy principles. A potential concern for large-scale implementation may be the cost of TBD; however, this limitation can be mitigated, as demonstrated by Fritz-Langhals, who developed a straightforward and cost-effective one-pot synthesis of a liquid TBD formulation.<sup>37</sup> Moreover, the generation of a single, benign by-product (TBD-HCl) enhances the process sustainability. As a guanidinium chloride, TBD-HCl has well-established applications in biochemistry, notably as a protein denaturant and nucleic acid stabilizer,<sup>52,53</sup> which supports its potential for recovery and reuse. To overcome current limitations in substitution efficiency, future work will explore process intensification strategies, such as flow chemistry, to improve both reaction kinetics and scalability. By bridging CO<sub>2</sub> utilization with PVC upcycling, this work contributes to the development of greener methodologies for the valorization of chlorine-rich polymers.

## Experimental

### Materials

Carbon dioxide N50 (≥99.999%) was supplied by Air Liquide. 1-Propanol (99+%), 1-butanol (≥99.4%, ACS reagent), 1-hexanol (anhydrous, ≥99%), deuterated chloroform (0.03 vol% TMS, deuteration degree min. 99.8% for NMR spectroscopy, stabilized with silver), 1-decanol (for synthesis), poly(vinyl chloride) (low molecular weight), as well as *N,N*-dimethylformamide (anhydrous, 99.8%) were purchased from Sigma-Aldrich. Methanol (GPR Rectapur) and octan-1-ol (purified) were purchased from VWR. 2-Butanone (or methyl ethyl ketone (MEK), ACS Reagent) was acquired from Acros Organics. Ethanol (denaturated with 3% diethylether, Desinfectol) was purchased from Chemlab. 1,5,7-Triazabicyclo[4.4.0]dec-5-ene (TBD) was supplied by Apollo Scientific. Deuterated tetrahydrofuran (99.5% D) was supplied by CortecNet. All reagents were used as received.

### Synthetic procedures

**General procedure for the synthesis of CO<sub>2</sub>BALs.** A Schlenk tube, equipped with a septum and a stir bar, is charged with a

mixture of TBD (1.3990 g, 0.01005 mol) and an alcohol (0.01005 mol or 0.03015 mol for methanol, and 0.05025 mol for ethanol and 1-propanol) in bulk. A butyl pipe is used to link the CO<sub>2</sub> tank and the Schlenk tube and a needle (20 G) is used to pierce the septum, allowing carbon dioxide ( $p_{\text{CO}_2} = 0.2$  bar) to be bubbled onto the reaction mixture in a continuous flow. For most CO<sub>2</sub>BOLs the reaction is performed at 90 °C in an oil bath and under 500 rpm stirring for 1 h 30. In the case of methanol, ethanol and 1-propanol, the reaction is performed at 50 °C in an oil bath.

$\delta_{\text{H}}$ (60 MHz; CDCl<sub>3</sub>; MeOCO<sub>2</sub><sup>-</sup>,TBD·H<sup>+</sup>) 3.59 (3H, s, MeOC(=O)O<sup>-</sup>), 3.29 (8H, dt, NCH<sub>2</sub>), 1.98 (4H, quint, CH<sub>2</sub>).

$\delta_{\text{H}}$ (60 MHz; CDCl<sub>3</sub>; EtOCO<sub>2</sub><sup>-</sup>,TBD·H<sup>+</sup>) 4.03 (2H, q, CH<sub>2</sub>OC(=O)O<sup>-</sup>), 3.29 (8H, dt, NCH<sub>2</sub>), 1.98 (4H, quint, CH<sub>2</sub>), 1.23 (3H, t, CH<sub>3</sub>).

$\delta_{\text{H}}$ (60 MHz; CDCl<sub>3</sub>; PrOCO<sub>2</sub><sup>-</sup>,TBD·H<sup>+</sup>) 3.87 (2H, q, CH<sub>2</sub>OC(=O)O<sup>-</sup>), 3.29 (8H, dt, NCH<sub>2</sub>), 1.98 (4H, quint, CH<sub>2</sub>), 1.57 (2H, quint, CH<sub>2</sub>), 0.94 (3H, t, Me).

$\delta_{\text{H}}$ (500 MHz; CDCl<sub>3</sub>; ButOCO<sub>2</sub><sup>-</sup>,TBD·H<sup>+</sup>) 3.91 (2H, q, CH<sub>2</sub>OC(=O)O<sup>-</sup>), 3.29 (8H, dt, NCH<sub>2</sub>), 1.98 (4H, quint, CH<sub>2</sub>), 1.59 (2H, quint, CH<sub>2</sub>), 1.40 (2H, m, CH<sub>2</sub>), 0.91 (3H, t, Me).

$\delta_{\text{H}}$ (500 MHz; CDCl<sub>3</sub>; HexOCO<sub>2</sub><sup>-</sup>,TBD·H<sup>+</sup>) 3.91 (2H, q, CH<sub>2</sub>OC(=O)O<sup>-</sup>), 3.29 (8H, dt, NCH<sub>2</sub>), 1.98 (4H, quint, CH<sub>2</sub>), 1.61 (2H, quint, CH<sub>2</sub>), 1.38 (2H, m, CH<sub>2</sub>), 1.28 (4H, m, (CH<sub>2</sub>)<sub>2</sub>CH<sub>3</sub>), 0.87 (3H, t, Me).

$\delta_{\text{H}}$ (500 MHz; CDCl<sub>3</sub>; OctOCO<sub>2</sub><sup>-</sup>,TBD·H<sup>+</sup>) 3.91 (2H, q, CH<sub>2</sub>OC(=O)O<sup>-</sup>), 3.30 (8H, dt, NCH<sub>2</sub>), 1.99 (4H, quint, CH<sub>2</sub>), 1.61 (2H, quint, CH<sub>2</sub>), 1.37 (2H, m, CH<sub>2</sub>), 1.27 (8H, m, (CH<sub>2</sub>)<sub>4</sub>CH<sub>3</sub>), 0.87 (3H, t, Me).

$\delta_{\text{H}}$ (500 MHz; CDCl<sub>3</sub>; DecOCO<sub>2</sub><sup>-</sup>,TBD·H<sup>+</sup>) 3.90 (2H, q, CH<sub>2</sub>OC(=O)O<sup>-</sup>), 3.30 (8H, dt, NCH<sub>2</sub>), 1.99 (4H, quint, CH<sub>2</sub>), 1.60 (2H, quint, CH<sub>2</sub>), 1.38 (2H, m, CH<sub>2</sub>), 1.25 (12H, m, (CH<sub>2</sub>)<sub>6</sub>CH<sub>3</sub>), 0.87 (3H, t, Me).

$\nu_{\text{max}}$ /cm<sup>-1</sup> 3232 (NH), 3152 (NH), 1655 (C=O), 1570 (C=N), 1388 (CO).

**General procedure for the reaction between CO<sub>2</sub>BALs and PVC.** PVC (0.01005 mol Cl, 0.6245 g PVC) was dissolved in MEK or DMF (20 ml). The CO<sub>2</sub>BAL (0.01005 mol) was then added to the solution. The reaction was performed at room temperature, under 500 rpm stirring, and CO<sub>2</sub> atmosphere for 0.5, 1, 2, 18 or 72 hours. After each reaction, the product is purified through a three step process. First, water is used to precipitate and wash the product. Then, the precipitate is solubilized in THF. Finally the solution from the previous step is precipitated in water, and the product is filtered, thoroughly washed with methanol and dried before analysis.

$\delta_{\text{H}}$ (500 MHz; THF-*d*<sub>8</sub>; modified PVC) 5.79 (2H, br t, CH=CH), 4.75 (1H, br t, CH<sub>2</sub>CHOC(=O)OC<sub>10</sub>H<sub>21</sub>), 4.49 (1H, br t, CH<sub>2</sub>CHCl), 4.09 (1H, br t, CH<sub>2</sub>CHOC(=O)OCH<sub>2</sub>C<sub>9</sub>H<sub>19</sub>), 2.24 (2H, br m, CH<sub>2</sub>CHCl, CH<sub>2</sub>CHOC(=O)OC<sub>10</sub>H<sub>21</sub>), 1.46 (2H, t, CH<sub>2</sub>CHOC(=O)OCH<sub>2</sub>CH<sub>2</sub>C<sub>8</sub>H<sub>17</sub>), 1.29 (14H, br m, CH<sub>2</sub>CHOC(=O)OCH<sub>2</sub>CH<sub>2</sub>(CH<sub>2</sub>)<sub>7</sub>CH<sub>3</sub>), 0.89 (3H, t, CH<sub>2</sub>CHOC(=O)O(CH<sub>2</sub>)<sub>9</sub>CH<sub>3</sub>).

$\nu_{\text{max}}$ /cm<sup>-1</sup> 1744 (C=O), 1429 (PVC), 1330 (PVC), 1250 (PVC), 1117 (C-O), 964 (PVC).

## Methods

**Melting point determination.** The general protocol was adapted from the one described in ref. 29. To that end, the melting point of each CO<sub>2</sub>BAL was determined visually by heating a pre-cooled sealed NMR tube containing CO<sub>2</sub>BAL compounds, at a rate of 1 °C per minute in an oil bath.

**Thermal stability – TGA and degradation kinetics.** CO<sub>2</sub>BALs were subjected to thermogravimetric analysis (TGA) to determine their degradation temperature. Measurements were performed under nitrogen flow at a rate of 5 °C per minute using a TA Q500 TGA.

Products of the reaction between CO<sub>2</sub>BAL and PVC were subjected to TGA as well. This allowed for thermal stability evaluation as well as the determination of the substitution rate. Measurements were performed under nitrogen flow at a rate of 2.5 °C per minute using a TA Q500 TGA.

In order to evaluate the CO<sub>2</sub>BALs' thermal stability, degradation kinetics analysis was performed. Samples were therefore subjected to a nitrogen flow ( $p(\text{N}_2) = 0.2$  bar) at different temperatures, using the same experimental setup as for their synthesis. Degradation was monitored regularly through <sup>1</sup>H NMR spectroscopy. The neperian logarithm of the degradation percentage was plotted against time. After linear regression, the slope obtained gave the kinetic constant of the degradation reaction ( $k$ ) at each temperature. Consequently, the plot of ln( $k$ ) against 1/ $T$  (K<sup>-1</sup>) allowed to work out the frequency factor ( $A$ ) and the activation energy ( $E_a$ ) parameters of the Arrhenius equation for the degradation reaction.

**FT-IR spectroscopy.** Fourier Transform InfraRed spectroscopy was performed using a Bruker Tensor 27 spectrometer to give an indication regarding the success of the substitution reaction between PVC and CO<sub>2</sub>BALs.

**NMR spectroscopy.** CO<sub>2</sub> conversion was followed time-to-time through <sup>1</sup>H nuclear magnetic resonance (NMR) using a Spinsolve 60 Ultrabenchttop NMR spectrometer (Magritek, Aachen, Germany). All spectra were acquired according to the following parameters: aq = 6.4 s, repetition time = 10 s, pulse angle = 90, ns = 32.

Final CO<sub>2</sub>BAL and substitution products were all characterized by <sup>1</sup>H NMR using a Bruker AVANCEII 500 MHz apparatus at room temperature in chloroform-*d*<sub>1</sub> (CDCl<sub>3</sub>) and THF-*d*<sub>8</sub>, respectively. All spectra were acquired according to the following parameters: aq = 6.8 s, d1 = 10 s, sw = 12, o1p = 5, ns = 32 for small molecules and 512 for PVC-based compounds.

**SEC.** Substitution products were subjected to size exclusion chromatography (SEC) in THF at 25 °C using a Triple Detection Polymer Laboratories liquid chromatograph equipped with a refractive index (ERMA 7517), a UV detector (254 nm), a capillary viscometry, a light scattering RALS (Viscotek T-60) (Polymer Laboratories GPC-RI/CV/RALS) and an automatic injector (Polymer Laboratories GPC-RI/UV) and four columns: a PL gel 10 μm guard column and three PL gel Mixed-B 10 μm columns (linear columns for separation of Mw PS ranging from 500 to 10<sup>6</sup> daltons). All samples for SEC ana-

lyses were prepared according to the following concentration: 1 mg of polymer sample in 1 mL of THF.

## Author contributions

Conceptualization: O. C.; methodology: J. D.; validation: J. D. and E. B. A.; investigation: J. D. and E. B. A.; writing – original draft: J. D.; writing – review & editing: O. C., J. D., and E. B. A.; visualization: J. D., E. B. A., and O. C.; supervision: O. C.

## Data availability

The data supporting this study, including spectroscopic, thermal, and chromatographic analyses, are available in the ESI† of this article. No additional datasets were generated or analyzed beyond those included in the main text and ESI.†

## Conflicts of interest

There are no conflicts to declare.

## Acknowledgements

J. D. and E. B. A. acknowledge the support of the AXA Research Fund for the funding of this project. O. C. acknowledges support for his position as a Senior Research Associate for the F.R.S.-FNRS of Belgium and AXA Professor in Chemistry.

## References

- 1 ChemAnalyst, *Poly Vinyl Chloride (PVC) Market Analysis: Industry Market Size, Plant Capacity, Production, Operating Efficiency, Demand & Supply, End-User Industries, Sales Channel, Regional Demand, Foreign Trade, Company Share, Manufacturing Process, 2015–2030*, ChemAnalyst, 2023.
- 2 The Circular economy for Plastics - A European Analysis, Plastics Europe, 2024.
- 3 A. Buekens and A. Sevenster, *J. Mater. Cycles Waste Manag.*, 2010, **12**, 184–192.
- 4 K. Lewandowski and K. Skórczewska, *Polymers*, 2022, **14**, 3035.
- 5 Z. Ait-Touchente, M. Khellaf, G. Raffin, N. Lebaz and A. Elaissari, *Polym. Adv. Technol.*, 2024, **35**, e6228.
- 6 M. Sadat-Shojai and G.-R. Bakhshandeh, *Polym. Degrad. Stab.*, 2011, **96**, 404–415.
- 7 X. Jiang, B. Zhu and M. Zhu, *Green Chem.*, 2023, **25**, 6971–7025.
- 8 D. E. Fagnani, D. Kim, S. I. Camarero, J. F. Alfaro and A. J. McNeil, *Nat. Chem.*, 2023, **15**, 222–229.
- 9 M. Liu, X. Wu and P. J. Dyson, *Nat. Chem.*, 2024, **16**, 700–708.
- 10 S. Mishra, S. Kar, R. Rangappa, P. Patil, V. Kadam, S. H. Chikkali and R. C. Samanta, *Chem. – Eur. J.*, 2025, **31**, e202403980.
- 11 J. L. S. Zackasee, V. Srivardhan, B. L. Truesdell, E. J. Vrana and C. S. Sevov, *Chem*, 2025, **11**, 102298.
- 12 S. Zhang, H. Han, M. Cao, Y. Xie and J. Chen, *Interdiscip. Mater.*, 2025, **4**, 5–23.
- 13 T. Yoshioka and G. Grause, in *Topical Themes in Energy and Resources*, ed. Y. Tanaka, M. Norton and Y.-Y. Li, Springer Japan, Tokyo, 2015, pp. 195–214.
- 14 S. Moulay, *J. Res. Updates Polym. Sci.*, 2015, **4**, 79–122.
- 15 S. Moulay, *Prog. Polym. Sci.*, 2010, **35**, 303–331.
- 16 R. K. Jha, B. J. Neyhouse, M. S. Young, D. E. Fagnani and A. J. McNeil, *Chem. Sci.*, 2024, **15**, 5802–5813.
- 17 Z. O. G. Schyns and M. P. Shaver, *Macromol. Rapid Commun.*, 2021, **42**, 2000415.
- 18 G. Martinez, N. Guarrotxena, J. M. Gomez-Elvira and J. Millan, *Polym. Bull.*, 1992, **28**, 427–433.
- 19 T. Kameda, M. Ono, G. Grause, T. Mizoguchi and T. Yoshioka, *Polym. Degrad. Stab.*, 2009, **94**, 107–112.
- 20 L. Shao, C. Qi and X.-M. Zhang, *RSC Adv.*, 2014, **4**, 53105–53108.
- 21 M. Bakherad, A. Keivanloo and S. Samangooei, *Chin. J. Catal.*, 2014, **35**, 324–328.
- 22 J. Zhu, Y. Su, X. Zhao, Y. Li, J. Zhao, X. Fan and Z. Jiang, *Ind. Eng. Chem. Res.*, 2014, **53**, 14046–14055.
- 23 A. Siekierka, J. Wolska, W. Kujawski and M. Bryjak, *Sep. Sci. Technol.*, 2018, **53**, 1191–1197.
- 24 S. Rabie, D. Ali, N. Khaireldin, M. El-Hashash, M. Elsaidi, A. El-Sayed and N. Wahed, *Egypt. J. Chem.*, 2020, **63**, 4833–4849.
- 25 E. J. Park, B. C. Park, Y. J. Kim, A. Canlier and T. S. Hwang, *Macromol. Res.*, 2018, **26**, 913–923.
- 26 N. G. Bush, M. K. Assefa, S. Bac, S. Mallikarjun Sharada and M. E. Fieser, *Mater. Horiz.*, 2023, **10**, 2047–2052.
- 27 L. Lu, S. Kumagai, T. Kameda, L. Luo and T. Yoshioka, *RSC Adv.*, 2019, **9**, 28870–28875.
- 28 G. Sneddon, J. C. McGlynn, M. S. Neumann, H. M. Aydin, H. H. P. Yiu and A. Y. Ganin, *J. Mater. Chem. A*, 2017, **5**, 11864–11872.
- 29 J. Delcorps, K. S. Rawat, M. Wells, E. Ben Ayed, B. Grignard, C. Detrembleur, B. Blankert, P. Gerbaux, V. Van Speybroeck and O. Coulembier, *Cell Rep. Phys. Sci.*, 2024, **5**, 102057.
- 30 D. J. Heldebrant, C. R. Yonker, P. G. Jessop and L. Phan, *Energy Procedia*, 2009, **1**, 1187–1195.
- 31 D. J. Heldebrant, C. R. Yonker, P. G. Jessop and L. Phan, *Energy Environ. Sci.*, 2008, **1**, 487–493.
- 32 D. J. Heldebrant, P. K. Koech, M. T. C. Ang, C. Liang, J. E. Rainbolt, C. R. Yonker and P. G. Jessop, *Green Chem.*, 2010, **12**, 713–721.
- 33 L. Phan, D. Chiu, D. J. Heldebrant, H. Huttenhower, E. John, X. Li, P. Pollet, R. Wang, C. A. Eckert, C. L. Liotta and P. G. Jessop, *Ind. Eng. Chem. Res.*, 2008, **47**, 539–545.
- 34 M. Verdecchia, M. Feroci, L. Palombi and L. Rossi, *J. Org. Chem.*, 2002, **67**, 8287–8289.

- 35 Á. Mesías-Salazar, R. S. Rojas, F. Carrillo-Hermosilla, J. Martínez, A. Antiñolo, O. S. Trofymchuk, F. M. Nachtigall, L. S. Santos and C. G. Daniliuc, *New J. Chem.*, 2024, **48**, 105–111.
- 36 S. G. Khokarale and J.-P. Mikkola, *RSC Adv.*, 2019, **9**, 34023–34031.
- 37 E. Fritz-Langhals, *Org. Process Res. Dev.*, 2022, **26**, 3015–3023.
- 38 Heat distortion temperature, <https://pvc.org/about-pvc/pvc-physical-properties/heat-distortion-temperature/>, (accessed 10 August 2024).
- 39 J. Yu, L. Sun, C. Ma, Y. Qiao and H. Yao, *Waste Manage.*, 2016, **48**, 300–314.
- 40 T. Moreno, P. Dyer and S. Tallon, *Ind. Eng. Chem. Res.*, 2020, **59**, 20307–20315.
- 41 G. Grause, A. Buekens, Y. Sakata, A. Okuwaki and T. Yoshioka, *J. Mater. Cycles Waste Manag.*, 2011, **13**, 265–282.
- 42 Z. Hou and R. M. Broughton, *J. Coated Fabr.*, 1998, **28**, 37–55.
- 43 S. Adanur, Z. Hou and R. M. Broughton, *J. Coated Fabr.*, 1998, **28**, 145–168.
- 44 G. Grause, S. Hirahashi, H. Toyoda, T. Kameda and T. Yoshioka, *J. Mater. Cycles Waste Manag.*, 2017, **19**, 612–622.
- 45 A. J. De Vries, C. Bonnebat and M. Carrega, *Pure Appl. Chem.*, 1971, **26**, 209–240.
- 46 A. Wirsén and P. Flodin, *J. Appl. Polym. Sci.*, 1978, **22**, 3039–3056.
- 47 S. Y. Lee, J. M. Murphy, A. Ukai and G. C. Fu, *J. Am. Chem. Soc.*, 2012, **134**, 15149–15153.
- 48 N. Choudhury, A. Kim, M. Kim and B.-S. Kim, *Adv. Mater.*, 2023, **35**, 2304113.
- 49 A. Salazar Avalos, M. Hakkarainen and K. Odelius, *Polymers*, 2017, **9**, 84.
- 50 P. Jia, M. Zhang, L. Hu, R. Wang, C. Sun and Y. Zhou, *Polymers*, 2017, **9**, 621.
- 51 E. Carrascosa, J. Meyer, J. Zhang, M. Stei, T. Michaelsen, W. L. Hase, L. Yang and R. Wester, *Nat. Commun.*, 2017, **8**, 25.
- 52 K. C. Aune and C. Tanford, *Biochemistry*, 1969, **8**, 4579–4585.
- 53 L. M. Mayr and F. X. Schmid, *Biochemistry*, 1993, **32**, 7994–7998.